Available online at www.sciencedirect.com
SCIENCE DIRECT®
ELSEVIER
Composites Science and Technology 63 (2003) 1655–1661
COMPOSITES SCIENCE AND TECHNOLOGY
www.elsevier.com/locate/compscitech

The stress–strain behavior of polymer–nanotube composites from molecular dynamics simulation

S.J.V. Frankland[a,*], V.M. Harik[b], G.M. Odegard[a], D.W. Brenner[c], T.S. Gates[d]

[a]National Institute of Aerospace, 144 Research Drive, Hampton, VA 23666, USA
[b]Swales Aerospace, M/S 186A, NASA Langley Research Center, Hampton, VA 23681, USA
[c]Department of Materials Science and Engineering, North Carolina State University, Raleigh, NC 27695, USA
[d]Mechanics and Durability Branch, M/S 188E, NASA Langley Research Center, Hampton, VA 23681, USA

Received 23 August 2002; received in revised form 1 November 2002; accepted 15 December 2002

Abstract

Stress–strain curves of polymer–carbon nanotube composites generated from molecular dynamics simulations of a single-walled carbon nanotube embedded in polyethylene are presented. A comparison is made between the response to mechanical loading of a composite with a long, continuous nanotube (replicated via periodic boundary conditions) and the response of a composite with a short, discontinuous nanotube. Both composites are mechanically loaded in the direction of, and transverse to, the nanotube axis. The long-nanotube composite shows an increase in the stiffness relative to the polymer and behaves anisotropically under the different loading conditions considered. The short-nanotube composite shows no enhancement relative to the polymer, most probably because of its low aspect ratio. The stress–strain curves from molecular dynamics simulations are compared with corresponding rule-of-mixtures predictions.
Published by Elsevier Ltd.

Keywords: A. Polymer-matrix composites (PMCs); B. Mechanical properties; B. Stress/strain curves; C. Computational simulation; Carbon nanotubes

1. Introduction

In the last few years, single-walled carbon nanotube-polymer composites have generated considerable interest in the materials research community because of their potential for large increases in strength and stiffness, when compared to conventional carbon-fiber-reinforced polymer composites. Even though some nanotube composite materials have been characterized experimentally [1–12], the development of these materials can be greatly facilitated by using computational methods that allow for parametric studies of the influence of material and geometry. In particular, molecular dynamics (MD) simulations can predict the effect of mechanical loading on specific regions of polymer–nanotube (NT) composites.

Various aspects of the mechanical reinforcement of polymers by carbon nanotubes (NT) have been addressed computationally. One example of recent work is an equivalent-continuum modeling method that was used to predict the elastic properties of two single-walled polyimide–NT composites for various NT volume fractions, lengths, and orientations [13]. At the continuum level, finite element analysis has been used to predict the macroscale effects of the waviness of NTs [14,15]. Molecular statics simulations of the transverse mechanical properties of NT bundles have shown that cohesion between NTs is strong, compared to a graphite–epoxy matrix [16]. Mechanical properties of NT yarns composed of twisted NT bundles have been predicted from the elastic constants of the NT bundles [17]. Molecular modeling has predicted the adhesion between a NT and various polymer matrices [18]. Molecular dynamics simulations have predicted that the polymer–NT interface can be reinforced by covalently bonding the NT to the polymer matrix [19].

The objective of this work is to explore the nanostructural effects of carbon NTs on the overall mechanical properties of polymer–NT composites. The overall

* Corresponding author. +Tel.: 1-757-864-4049; fax: +1-757-766-1855.
E-mail addresses: sjvf@nianet.org (S.J.V. Frankland).

0266-3538/03/$ - see front matter Published by Elsevier Ltd.
doi:10.1016/S0266-3538(03)00059-9

Nomenclature

A_1, A_2, A_3	constants for torsional potential $\phi(\theta)$
A_{cell}	cross-sectional area of unit cell
E	total internal energy of solid
E^{α}	total internal energy of atom α
f_{NT}	nanotube volume fraction
f_m	polymer matrix volume fraction
$F_i^{\alpha\beta}$	*i*-component of the force between atoms α and β
h_{vdW}	average van der Waals separation distance between nanotube and matrix
M^{α}	mass of atom α
S	denotes constant entropy
T^{α}	kinetic energy of atom α
U^{α}	potential energy of atom α
r	magnitude of separation distance between a pair of atoms
$r_j^{\alpha\beta}$	*j*-component of the separation distance of atoms α and β
R_{NT}	radius of nanotube
U	potential energy between a pair of atoms
V	volume of solid
V^{α}	atomic volume of atom α
Y_1	longitudinal elastic modulus of composite
Y_{1NT}	elastic modulus of nanotube
Y_2	transverse elastic modulus of composite
Y_{2NT}	effective transverse elastic modulus of nanotube
Y_m	elastic modulus of the polymer matrix
ε_{ij}	strain tensor
ε_{LJ}	potential well depth
$\phi(\theta)$	torsional potential for angle θ
$\Phi^{\alpha}(r)$	potential energy at the atom α for separation distance r
v^{α}	magnitude of the velocity of atom α
v_i^{α}	*i*-component of the velocity of atom α
θ	torsional angle around the CH_2–CH_2 bond
σ_{ij}	stress tensor
σ_{LJ}	van der Waals separation distance

mechanical response of NT–polymer composites when subjected to mechanical loading is provided by the stress–strain relationship. In the present work, stress–strain curves of two unidirectional polyethylene–NT composites are presented that are generated from molecular dynamics simulations [20]. The effects of both the anisotropy of the composites, when subjected to different loading conditions, and of the length of the NT are demonstrated by examining two different configurations. The first composite unit cell contains a long (infinitely long) NT, and the second composite uncil cell contains a short (discontinuous) NT. In the following discussion, details of the composite structure and MD simulations are presented first. Then, a detailed description of the computation of stress from molecular force fields is given. Next, a rule-of-mixtures analysis, that is used for comparison with the stress–strain curves generated by MD simulation, is described. Finally, the stress–strain curves generated from MD simulation are presented for longitudinal and transverse loading conditions for each of the two composites considered.

2. Molecular dynamics simulations

The unidirectional NT–polymer composites considered in this work contain symmetrically placed long or short NTs, as shown in Fig. 1. The dashed boxes in Fig. 1 enclose a representative volume element that is simulated by MD. In each composite, the NTs are sufficiently separated by polymer to prevent direct NT–NT interactions. The NT composite in Fig. 1(a) contains a periodically replicated (10,10) NT which spans the length of the simulation cell. The (*n*,*m*) notation refers to the chiral vector of the NT in terms of the primitive in-plane lattice vectors of a graphene sheet [21]. In this composite, the NT is embedded in an amorphous polyethylene (PE) matrix, which is represented by beads of united atom –CH_2– units. Specifically, the PE matrix has eight chains of 1095 –CH_2– units. The short-NT composite, shown in Fig. 1(b), contains a 6-nm capped

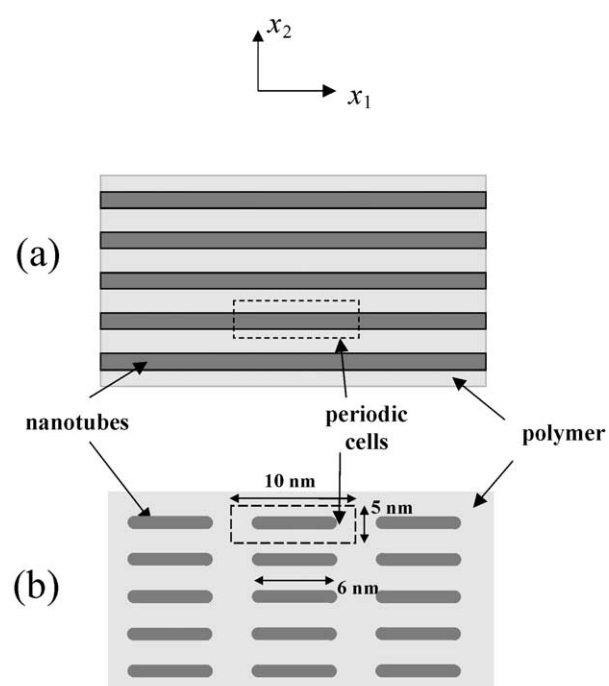

Fig. 1. Schematic of polymer nanocomposites filled with long and short carbon nanotubes.

(10,10) NT which is approximately half the length of the simulation cell. The NT caps each consist of one half of a C_{240} molecule. In this composite, the amorphous PE matrix contains eight chains of 1420 $-CH_2-$ units. The overall dimensions for the unit-cell, or minimum image, of each composite in the MD simulation are approximately $5\times5\times10$ nm. Periodic boundary conditions were used to replicate the cell in all three dimensions. For comparison to the NT/PE composites, an equivalent-sized block of amorphous PE without a NT was also simulated. For each structure, a PE density of 0.71 g/cm^3 was used.

In the MD simulation, the van der Waals interfacial interaction between the polymer and the NT was modeled with the Lennard–Jones potential [22],

$$U = 4\varepsilon_{LJ}\left(\frac{\sigma_{LJ}^{12}}{r^{12}} - \frac{\sigma_{LJ}^{6}}{r^{6}}\right) \quad (1)$$

where U is the potential energy between a pair of atoms, r is the separation distance between the pair of atoms, ε_{LJ} is the potential well depth, and σ_{LJ} is the van der Waals separation distance. For the interaction between the carbon atoms of the NT and the polymer $-CH_2-$ units, the potential was parametrized with $\varepsilon_{LJ} = 0.4492$ kJ/mol and $\sigma_{LJ} = 0.3825$ nm [22,23]. The PE chains were simulated with a molecular-mechanics force field adapted from Ref. [23]. Specifically, the $-CH_2-$ units of the PE chains were separated by bond lengths of 0.153 nm by using the SHAKE algorithm, a constraint dynamics method which constrains the bond length within a user-defined tolerance [22]. Angle bending forces were modeled with a harmonic valence-angle potential having an equilibrium angle of 112.813° and a barrier of 520 kJ/mol. A torsional potential $\phi(\theta)$ of the form

$$\phi(\theta) = A_1(1+\cos\theta) + A_2(1+\cos2\theta) + A_3(1+\cos3\theta) \quad (2)$$

was used where θ is the torsional angle around the CH_2–CH_2 bond, and $A_1 = -18.087$, $A_2 = -4.88$, and $A_3 = 31.8$ kJ/mol [23]. The Lennard–Jones potential was also used to describe non-bonding interactions between $-CH_2-$ units in either the same chain or between different chains. For these interactions, $\varepsilon_{LJ} = 0.4742$ kJ/mol and $\sigma_{LJ} = 0.428$ nm [23]. The NT was modeled with a many-body bond-order potential developed for carbon [24]. This carbon potential is parametrized for C–C bonds of lengths up to 0.17 nm, which is within the magnitude of the strain applied to the composites in the present work.

The MD simulations were carried out by using DL-POLY [25], a large-scale MD simulation package available from Daresbury Laboratory. This program was adapted to include the carbon potential for the NT and to simulate the application of strain to the composite. All simulations were carried out at 300 K, with a 2 fs time step.

3. Stress–strain curves from simulation

Stress–strain curves were generated for the long- and short-NT composites and for the pure polymer via MD simulation. For both composite configurations, the longitudinal (parallel to the NT axis) and transverse responses were simulated.

3.1. Strain

For each increment of applied deformation, a uniform strain was prescribed on the entire MD model. For the longitudinal and transverse deformations, pure states of the strains ε_{11} and ε_{22}, respectively, were initially applied (see Fig. 2). The application of strain was accomplished by uniformly expanding the dimensions of the MD cell in the direction of the deformation and re-scaling the new coordinates of the atoms to fit within the new dimensions. After this initial deformation, the MD simulation was continued and the atoms were allowed to equilibrate within the new MD cell dimensions. This process was

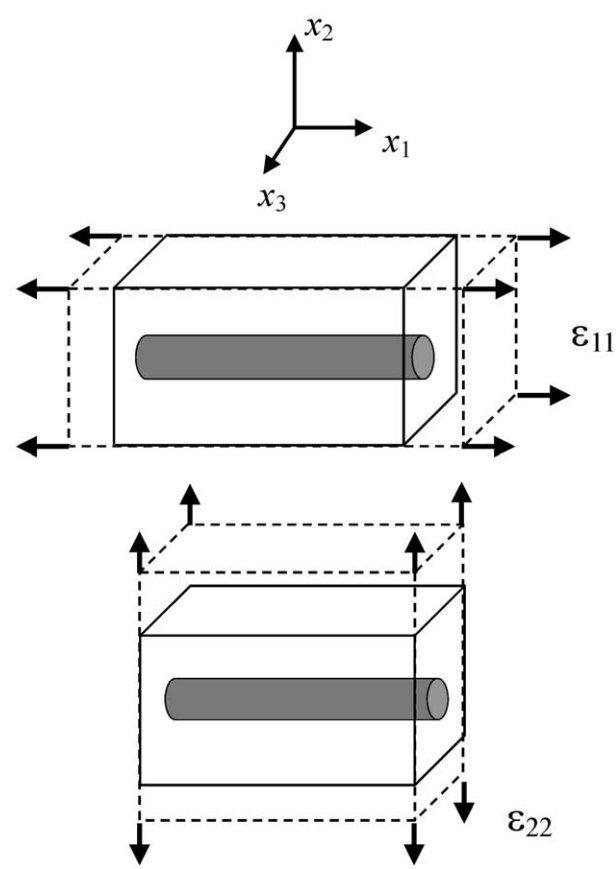

Fig. 2. Definitions of the strains applied to the composites.

carried out for the subsequent increments of deformation. The applied-strain increment, in either the longitudinal or transverse direction, was 2%, and was applied in two equal increments of 1% each 1 ps (500 steps) apart. After each 2% increment of strain, the system was relaxed for 2 ps, then the stress on the system was averaged over an interval of 10 ps. For each composite configuration, six increments of 2% strain were applied up to a total of approximately 12% over a period of 72 ps. The corresponding strain rate was 1.0×10^{10} s^{-1}. This high strain rate is inherent to MD simulation which includes dynamical information usually on ps or ns timescales.

3.2. Stress

In general, the stress in a solid (or a group of interacting particles in the form of a solid) is defined as the change in the internal energy (in the thermodynamic sense) with respect to the strain per unit volume. For example, at the continuum level, the stress tensor, σ_{ij}, for a linear-elastic material is [26]

$$\sigma_{ij} = \frac{1}{V}\left(\frac{\partial E}{\partial \varepsilon_{ij}}\right)_S \tag{3}$$

where V is the volume of the solid, E is the total internal energy, ε_{ij} is the strain tensor, and the subscript S denotes constant entropy. When the internal energy is equal to the strain energy of the solid, then Hooke's law may be derived from Eq. (3). Furthermore, if the strain energy is expressed in terms of an applied force acting over the surface area of a solid, then a more familiar form of stress as force per unit area is derived.

At the atomic level, the total internal energy given in Eq. (3) can be expressed as the summation of the energies of the individual atoms, E^α, that compose the solid:

$$E^\alpha = T^\alpha + U^\alpha = \frac{1}{2}M^\alpha(v^\alpha)^2 + \Phi^\alpha(r) \tag{4}$$

where for each atom α, T^α is the kinetic energy, U^α is the potential energy, M^α is the mass, v^α is the magnitude of its velocity, and $\Phi^\alpha(r)$ is the potential energy at the atom location r. Using a Hamiltonian based on these individual energy contributions, E^α, it has been shown that the stress contribution, σ_{ij}^α, for a given atom is

$$\sigma_{ij}^\alpha = -\frac{1}{V^\alpha}\left(M^\alpha v_i^\alpha v_j^\alpha + \sum_\beta F_i^{\alpha\beta} r_j^{\alpha\beta}\right) \tag{5}$$

where V^α is the atomic volume of atom α, v_i^α is the i-component of the velocity of atom α, v_j^α is the j-component of the velocity of atom α, $F_i^{\alpha\beta}$ is the i-component of the force between atoms α and β obtainable from the derivative of the potential $\Phi(r)$, and $r_j^{\alpha\beta}$ is the j-component of the separation of atoms α and β [27,28]. These parameters are shown in Fig. 3 as well.

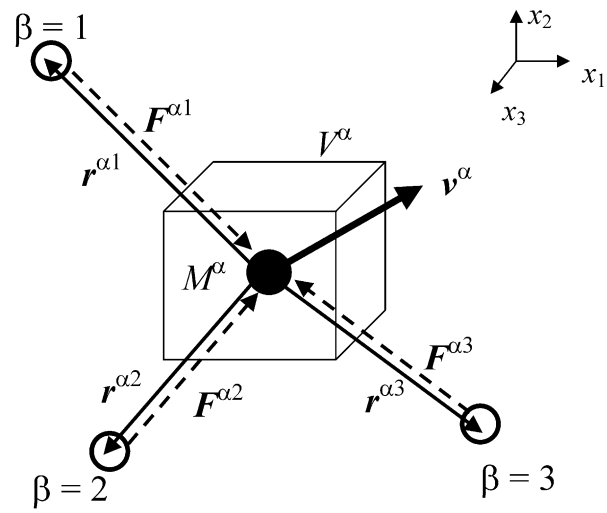

Fig. 3. Diagram of parameters used to compute stresses in the simulation.

The stresses that were used to generate the stress–strain curves for the NT composites were average atomic stresses for the volume of the model. Therefore, the stress components of each model were calculated for each strain increment by using

$$\sigma_{ij} = -\frac{1}{V}\sum_\alpha\left(M^\alpha v_i^\alpha v_j^\alpha + \sum_\beta F_i^{\alpha\beta} r_j^{\alpha\beta}\right) \tag{6}$$

where V is the volume of the MD model and $V = \sum_\alpha V^\alpha$. The stress calculated with Eq. (6) was then averaged over time via the MD simulation.

4. Rule-of-mixtures analysis

For a nanocomposite under uniaxial loading, the dependence of the elastic modulus on the NT volume fraction can be estimated by the rule of mixtures [29]. The longitudinal elastic modulus, Y_1, of the composite cell with long NTs under constant-strain conditions is

$$Y_1 = Y_{1\mathrm{NT}} f_{\mathrm{NT}} + Y_{\mathrm{m}} f_{\mathrm{m}} \tag{7}$$

where $Y_{1\mathrm{NT}}$ and Y_{m} are the effective longitudinal elastic modulus of the NT and the polymer matrix, respectively, and f_{NT} and f_{m} are the volume fractions occupied by the NT and the polymer matrix, respectively. The transverse modulus of the nanocomposite, Y_2, is

$$\frac{1}{Y_2} = \frac{f_{\mathrm{NT}}}{Y_{2\mathrm{NT}}} + \frac{f_{\mathrm{m}}}{Y_{\mathrm{m}}} \tag{8}$$

where $Y_{2\mathrm{NT}}$ is the effective elastic modulus of a NT in the transverse direction. The volume fractions satisfy

$$f_{\mathrm{NT}} + f_{\mathrm{m}} = 1. \tag{9}$$

The (10,10) NT used in the present work has a radius small enough to allow it to be treated as a solid beam [30]. Therefore, its volume fraction, f_{NT}, includes the entire NT cross-section and is given by

$$f_{NT} = \frac{\pi\left(R_{NT} + \frac{h_{vdW}}{2}\right)^2}{A_{cell}} \tag{10}$$

where h_{vdW} is the equilibrium van der Waals separation distance between the NT and the matrix, and A_{cell} is the cross-sectional area of the unit cell. The van der Waals separation distance depends on the nature of the polymer–NT interfacial interactions.

5. Results and discussion

The stress–strain curves of the long- and short-NT composites generated from MD simulation are presented in Figs. 4–6. Before describing the individual stress–strain curves in more detail, some general comments are in order. First, the endpoints of the curves are indicative of how far the simulation was conducted, and hence, should not be taken as yield points. No attempt is made in this work to simulate the yielding of the carbon nanotubes. Also, for both composite configurations, the maximum strains are on the order of 10% after the unit cell has been subjected to the stepwise increases of applied strain, as described in Section 3.1. The strain leads to an overall displacement of 0.5 nm for each unit-cell edge in the longitudinal direction and 0.25 nm in the transverse direction.

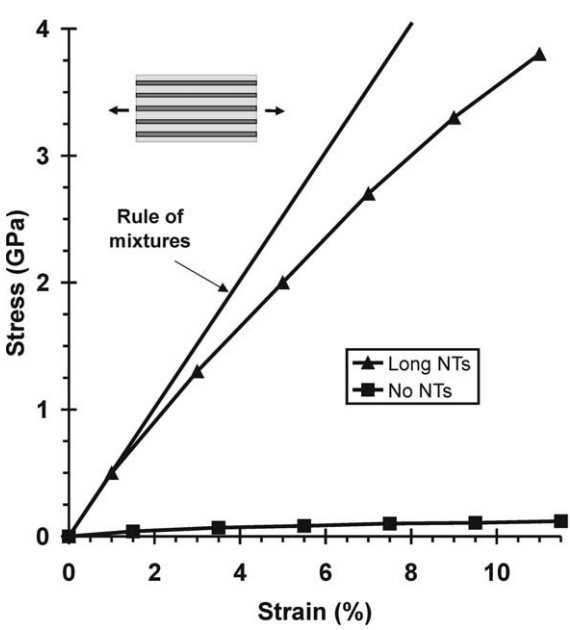

Fig. 4. Longitudinal stress–strain relation of long-NT composite and the results from the rule of mixtures. The stress–strain relation of the polymer matrix without nanotubes is included for comparison.

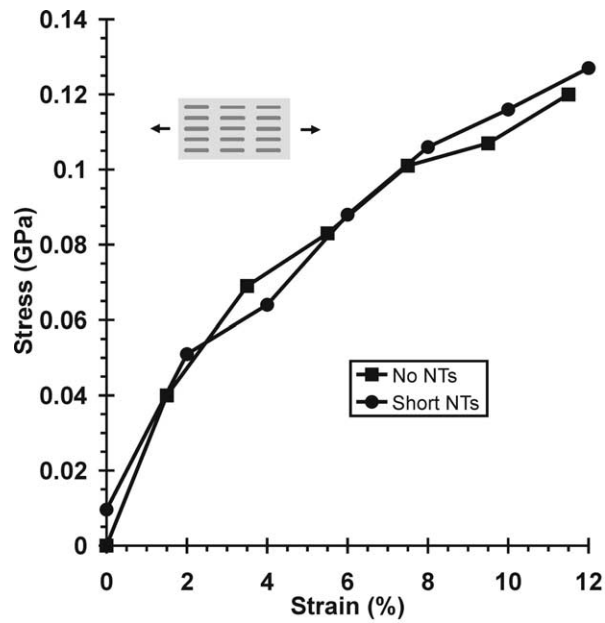

Fig. 5. Longitudinal stress–strain relation for the short NT-fitted composite compared with the stress–strain behavior of the polymer matrix without nanotubes

In Fig. 4, the stress–strain curve (solid triangles on solid line) of the long-NT composite under longitudinal loading conditions is compared with results calculated from the rule of mixtures (solid line without symbols) from Eq. (7). Of the composites simulated here, this one has the most significant enhancement in its stress–strain curve relative to the polymer (solid squares on solid line). For this sample, both the NT and the polymer

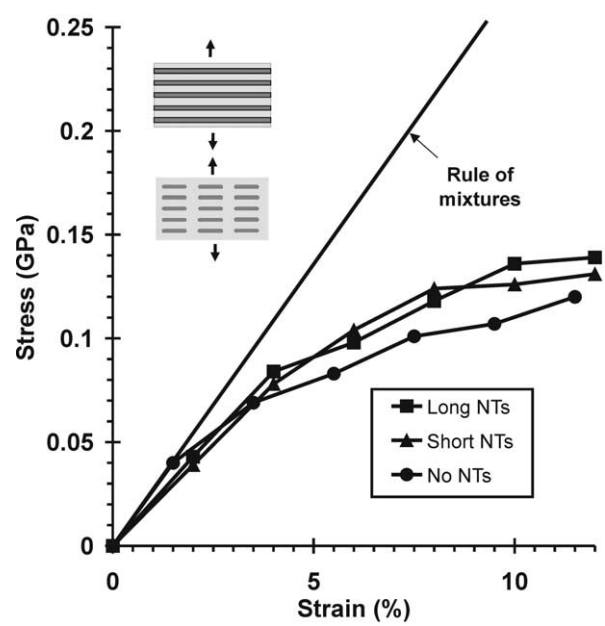

Fig. 6. Transverse stress–strain curves of both long and short NT-filled composites compared with polymer matrix without nanotubes and the results from the transverse rule of mixtures for the long NT-filled composite.

were subjected to constant-strain conditions. The stress–strain curve is comparable at low strain to the stress-strain behavior predicted by the rule of mixtures in Eq. (7), using a volume fraction of 8%, which is the NT volume fraction in the simulated composite, and an effective modulus of 600 GPa for the (10,10) NT [31].

The stress–strain curve of the short-NT (solid circles on solid line) subjected to longitudinal loading conditions is plotted with the simulated polymer stress–strain curve (solid squares on solid line) in Fig. 5. Almost no enhancement relative to the polymer is observed in the stress–strain curve of the composite with the short 6-nm NT. The bulk polymer stiffness is improved by less than a factor of two when the NTs are added into the polymer. This lack of effect is consistent with the low aspect ratio of the nanotube, 1:4, which is considerably lower than the more than 1:1000 aspect ratio expected for a typical single-walled NT. Furthermore, the simulated interface is established by non-bonding van der Waals forces between the polymer and the carbon NT [32], and there are no chemical bonds [19] or other strong interactions [13] to strengthen the interfacial adhesion.

The stress–strain curves of both composites subjected to transverse loading conditions are compared with each other and the polymer (solid circles on solid line) in Fig. 6. All three MD generated curves are similar. For the composite with the long NT (solid squares on solid line), the stress after loading in the transverse direction is approximately 30 times lower than the stress levels after loading to the same strain level in the longitudinal direction (Fig. 4). This difference in longitudinal and transverse behavior illustrates the anisotropy of the composite. Both the long- and short-NT composites exhibit similar transverse behavior relative to that of the polymer, which may be because the NT fills the same relative cross-sectional area in both composites. The solid line in Fig. 6 is calculated from the transverse rule of mixtures given by Eq. (8) for transverse loading conditions of the long-NT composite. For this comparison, an effective NT transverse modulus of 10 GPa [33] is used, and a polymer modulus of 2.7 GPa, which is derived from the initial points of the simulated polymer stress–strain curve. For somewhat higher estimates of the NT transverse modulus, the predictions will not change because the contribution from the matrix modulus is dominant in Eq. (8).

6. Concluding remarks

Molecular dynamics (MD) simulations were used to generate the stress-strain behavior of polymer-carbon nanotube (NT) composites mechanically loaded in both the longitudinal and transverse directions. Two NT geometries, long continuous fibers and short discontinuous fibers, were investigated. Stress at the atomic level was defined by using energy considerations, averaged over the volume of the MD model. The simulated stress-strain curves were compared with results calculated from the rule of mixtures.

The stiffest behavior, and the one closest to approaching the stiffness obtained by using the rule of mixtures, was observed for the longitudinally loaded, long continuous NT composite. This highly anisotropic composite, when subjected to transverse loading conditions, showed stresses that were more than one order of magnitude lower than those developed when it was subjected to longitudinal loading conditions. In contrast, the short, discontinuous fiber composite, upon loading in either direction, showed no appreciable load transfer from the polymer to the NT. An increase in the aspect ratio of the NT in this composite is anticipated to lead to further enhancement of the stress–strain curve and greater differences between the longitudinal and transverse stress–strain behavior [19,34].

Acknowledgements

The authors thank S.B. Sinnott, O.A. Shenderova, and S.P. Adiga for helpful discussions. Support from a Multi-University Research Initiative of the Office of Naval Research through the North Carolina Center for Nanoscale Materials is gratefully acknowledged by S.J.V. Frankland and D.W. Brenner. This research was partially supported by the National Aeronautics and Space Administration under NASA Contract No. NAS1-97046 while S.J.V. Frankland, V.M. Harik, and G.M. Odegard were at ICASE, NASA Langley Research Center. The simulations were carried out with facilities at the North Carolina Supercomputing Center.

References

[1] Schadler LS, Giannaris SC, Ajayan PM. Load transfer in carbon nanotube epoxy composites. Appl Phys Lett 1998;73:3842–4.
[2] Ajayan PM, Schadler LS, Giannaris SC, Rubio A. Single-walled carbon nanotube-polymer composites: strength and weakness. Adv Materials 2000;12:750–3.
[3] Gong X, Liu J, Baskaran S, Voise RD, Young JS. Surfactant-assisted processing of carbon nanotube/polymer composite. Chem Mater 2000;12:1049–52.
[4] Haggenmueller R, Gommans HH, Rinzler AG, Fischer JE, Winey KI. Aligned single-wall carbon nanotubes in composites by melt processing methods. Chem Phys Lett 2000;330:219–25.
[5] Qian D, Dickey EC, Andrews R, Rantell T. Load transfer and deformation mechanisms in carbon nanotube-polystyrene composites. Appl Phys Lett 2000;76:2868–70.
[6] Shaffer MSP, Windle AH. Fabrication and characterization of carbon nanotube/poly(vinyl alcohol) composites. Adv Materials 1999;11:937–41.
[7] Jin L, Bower C, Zhou O. Alignment of carbon nanotubes in a polymer matrix by mechanical stretching. Appl Phys Lett 1998; 73:1197–9.

[8] Bower C, Rosen R, Jin L, Han J, Zhou O. Deformation of carbon nanotubes in nanotube-polymer composites. Appl Phys Lett 1999;74:3317–9.
[9] Wagner HD, Lourie O, Feldman Y, Tenne R. Stress-induced fragmentation of multiwall carbon nanotubes in a polymer matrix. Appl Phys Lett 1998;72:188–90.
[10] Lourie O, Wagner HD. Transmission electron microscopy observations fracture of single-wall carbon nanotubes under axial tension. Appl Phys Lett 1998;73:3527–9.
[11] Lamy de la Chapelle M, Stephan C, Nguyen TP, Lefrant S, Journet C, Bernier P, et al. Raman characterization of single-walled carbon nanotubes and PMMA-nanotubes composites. Synthetic Metals 1999;103:2510–2.
[12] Jia Z, Wang Z, Xu C, Liang J, Wei B, Wu D, et al. Study on poly(methyl methacrylate)/carbon nanotube composites. Mat Sci Eng A 1999;271:395–400.
[13] Odegard G M, Gates T S, Wise K, Park C, Siochi E J. Constitutive modeling of nanotube reinforced polymer composites. Comp Sci Tech [submitted for publication].
[14] Fisher F T, Bradshaw R D, Brinson L C. Fiber waviness in nanotube-reinforced polymer composites: I. Modulus predictions using effective nanotube properties, Comp Sci Tech [submitted for publication].
[15] Bradshaw R D, Fisher F T, Brinson L C. Fiber waviness in nanotube-reinforced polymer composites II. Modeling via numerical approximation of the dilute strain concentration tensor. Comp Sci Tech [submitted for publication].
[16] Saether E, Frankland S J V, Pipes R B. Transverse mechanical properties of single-walled carbon nanotube crystals. Comp Sci Tech [submitted for publication].
[17] Pipes RB, Hubert P. Helical carbon nanotube arrays: Mechanical properties. Comp Sci Techn 2002;62:419–28.
[18] Lordi V, Yao N. Molecular mechanics of binding in carbon nanotube-polymer composites. J Mater Res 2000;15:2770–9.
[19] Frankland SJV, Caglar A, Brenner DW, Griebel M. Molecular simulation of the influence of chemical cross-links on the shear strength of carbon nanotube-polymer interfaces. J Phys Chem B 2002;106:3046–9.
[20] Frankland SJV, Brenner DW. Molecular dynamics simulations of polymer-nanotube composites. In: Sullivan JP, Robertson J, Zhou O, Allen TB, Coll BF, editors. Amorphous and Nanostructured Carbon. Mat. Res. Soc. Symp. Proc., 593. Warrendale, PA; 1999. p. 199–204.
[21] Dresselhaus MS, Dresselhaus G, Eklund PC. Science of fullerenes and carbon nanotubes. New York: Academic Press; 1996.
[22] Allen MP, Tildesley DJ. Computer simulation of liquids. Oxford: Clarendon Press; 1987.
[23] Clarke J H R. In: Binder K, editor. Monte Carlo and molecular dynamics in polymer sciences. New York: Oxford University Press; 1995. p. 272.
[24] Brenner DW, Shenderova OA, Harrison JA, Stuart SJ, Ni B, Sinnott SB. Second generation reactive empirical bond order (REBO) potential energy expression for hydrocarbons. J Phys C: Cond Matter 2002;14:783.
[25] DL-POLY is a package of molecular simulations subroutines written by W Smith and T R Forester, copyright The Council for the Central Laboratory of the Research Councils, Daresbury Laboratory at Daresbury, Nr. Warrington, England, UK, 1996.
[26] Fung CY. Foundations of solid mechanics. Englewood Cliffs (NJ): Prentice-Hall; 1965.
[27] Nielsen OH, Martin RM. Quantum-mechanical theory of stress and force. Phys Rev B 1985;32:3780–91.
[28] Vitek V, Egami T. Atomic level stresses in solids and liquids, Phys. Stat Solidi B: Basic Research 1987;144:145–56.
[29] Tsai SW. Composites design. Dayton OH: Think Composites Press; 1988.
[30] Harik VM. Ranges of applicability for the continuum beam model in the mechanics of carbon nanotubes and nanorods. Solid State Commun 2001;120:331–5.
[31] Cornwell CF, Wille LT. Elastic properties of single-walled carbon nanotubes in compression. Solid State Commun 1997;101:555–8.
[32] Frankland SJV, Caglar A, Brenner DW, Griebel M. Reinforcement mechanisms in polymer nanotube composites: simulated non-bonded and cross-linked systems. In Rao AM, editor. Nanotubes and Related Materials. Mat. Res. Soc. Symp. Proc., 633, Warrendale, PA, 2000, P.A.14.17. 1–5
[33] Popov VN, Van Doren VE, Balkanski M. Elastic properties of crystals of single-walled carbon nanotubes. Solid State Commun 2000;114:395–9.
[34] Kelly A, MacMillan NH. Strong solids. 3rd ed. Oxford: Clarendon Press; 1986.